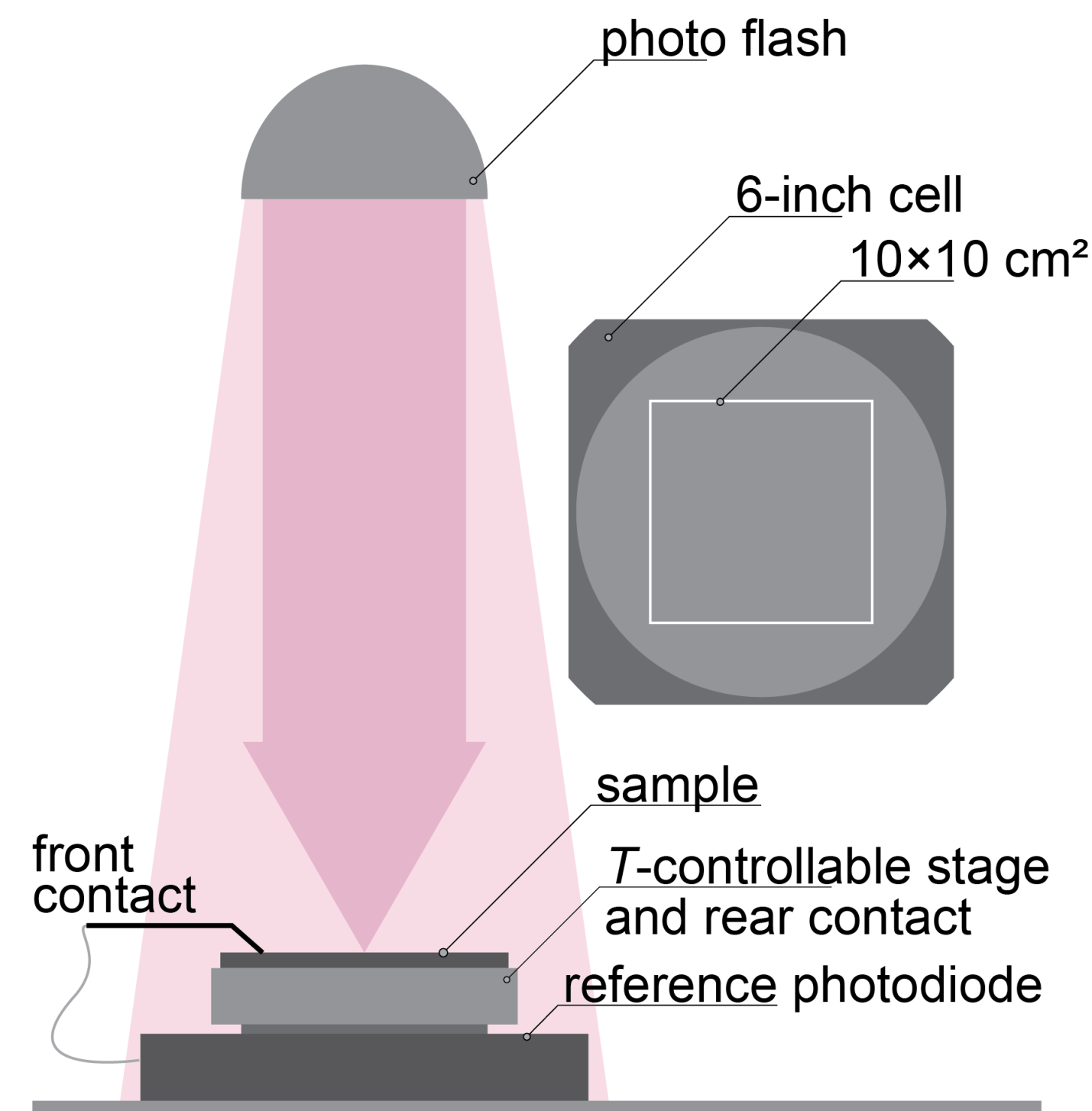


## Introduction

- Knowledge regarding the temperature and illumination dependence of solar cell performance is essential for their optimization and for the prediction of the power output from photovoltaic systems.
- It is required to understand benefits and limitations of different cell technologies in diverse operating conditions, when selecting modules for a specific location.
- In this study, we (1) introduce an advanced characterization tool - the temperature-dependent  $Suns-V_{oc}$  [ $Suns-V_{oc}(T)$ ], (2) apply this characterization method to different cell structures, and (3) compare results obtained by  $Suns-V_{oc}(T)$  and  $I-V(T)$ .

## Methodology



**Fig. 1.** Sketch of the temperature-dependent  $Suns-V_{oc}$  tool.

$Suns-V_{oc}(T)$  system allows measurement of both the temperature (from 25 to 200 °C) and illumination (from  $10^{-3}$  to  $10^2$  suns) dependence of solar cells.

## Results and discussion

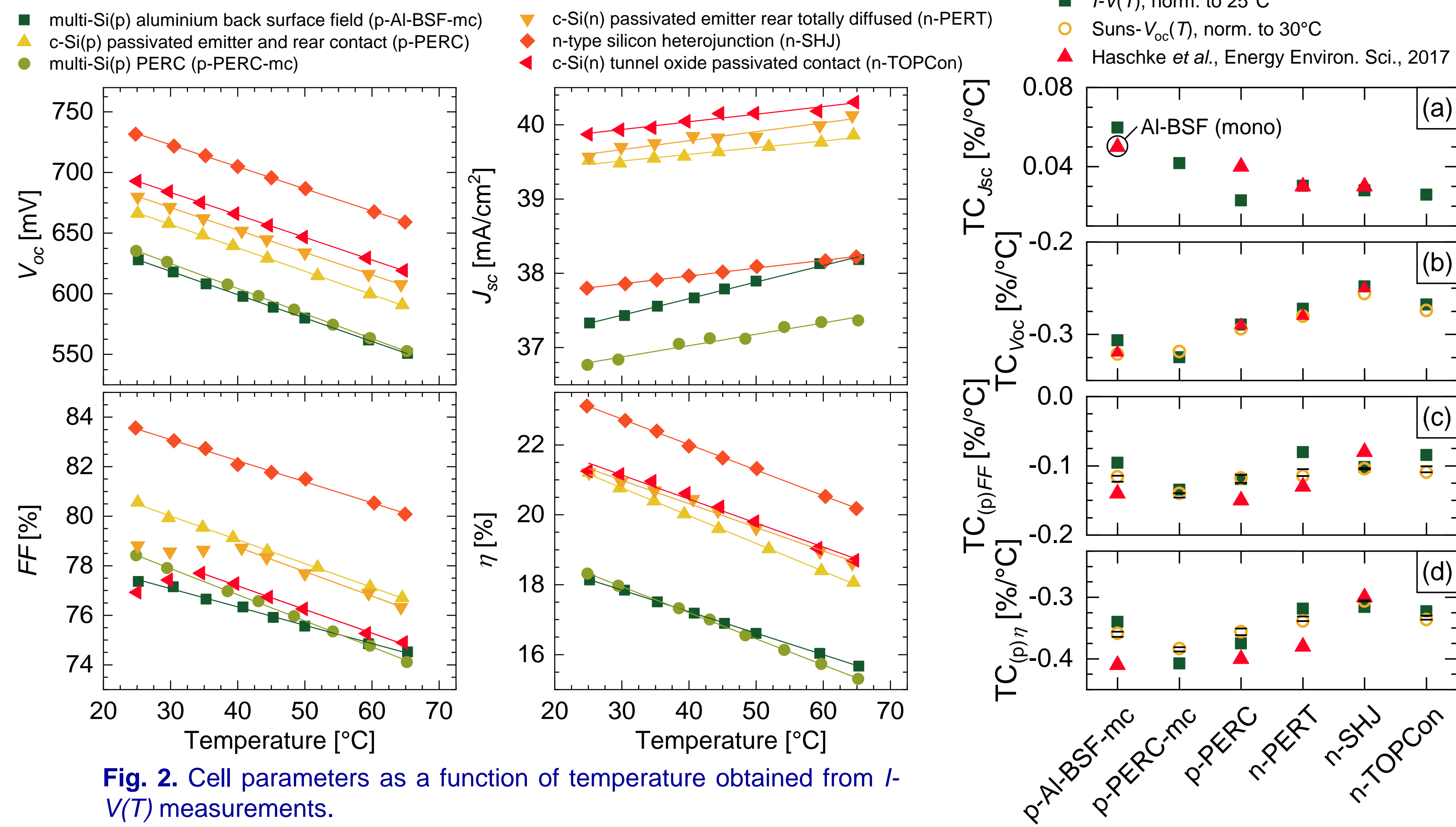


**Fig. 2.** Cell parameters as a function of temperature obtained from  $I-V(T)$  measurements.

- As expected, with increasing temperature:
  - The open-circuit voltage ( $V_{oc}$ ) and the fill factor ( $FF$ ) drop due to an increase of the effective intrinsic carrier concentration.
  - The short circuit-current density ( $J_{sc}$ ) increases due to band gap narrowing.
  - The cell efficiency ( $\eta$ ), dominated by  $V_{oc}$ , decreases as well.
- Passivating contact cell structures, *i.e.* SHJ and TOPCon, show better  $V_{oc}$  and efficiency across the entire temperature range.

## Conclusions

- $Suns-V_{oc}(T)$  enables the analysis of the temperature and illumination dependence of the cell performance simultaneously.
- Passivating contact cell structures, *i.e.* SHJ and TOPCon, show better  $TC_{V_{oc}}$  compared to the ones without passivating contacts.
- The investigated cells are more sensitive to temperature variation at lower illumination intensities.
- $m(V)$  at different operating temperatures obtained by  $Suns-V_{oc}(T)$  distinguishes the resistance and dark saturation current density related effects.

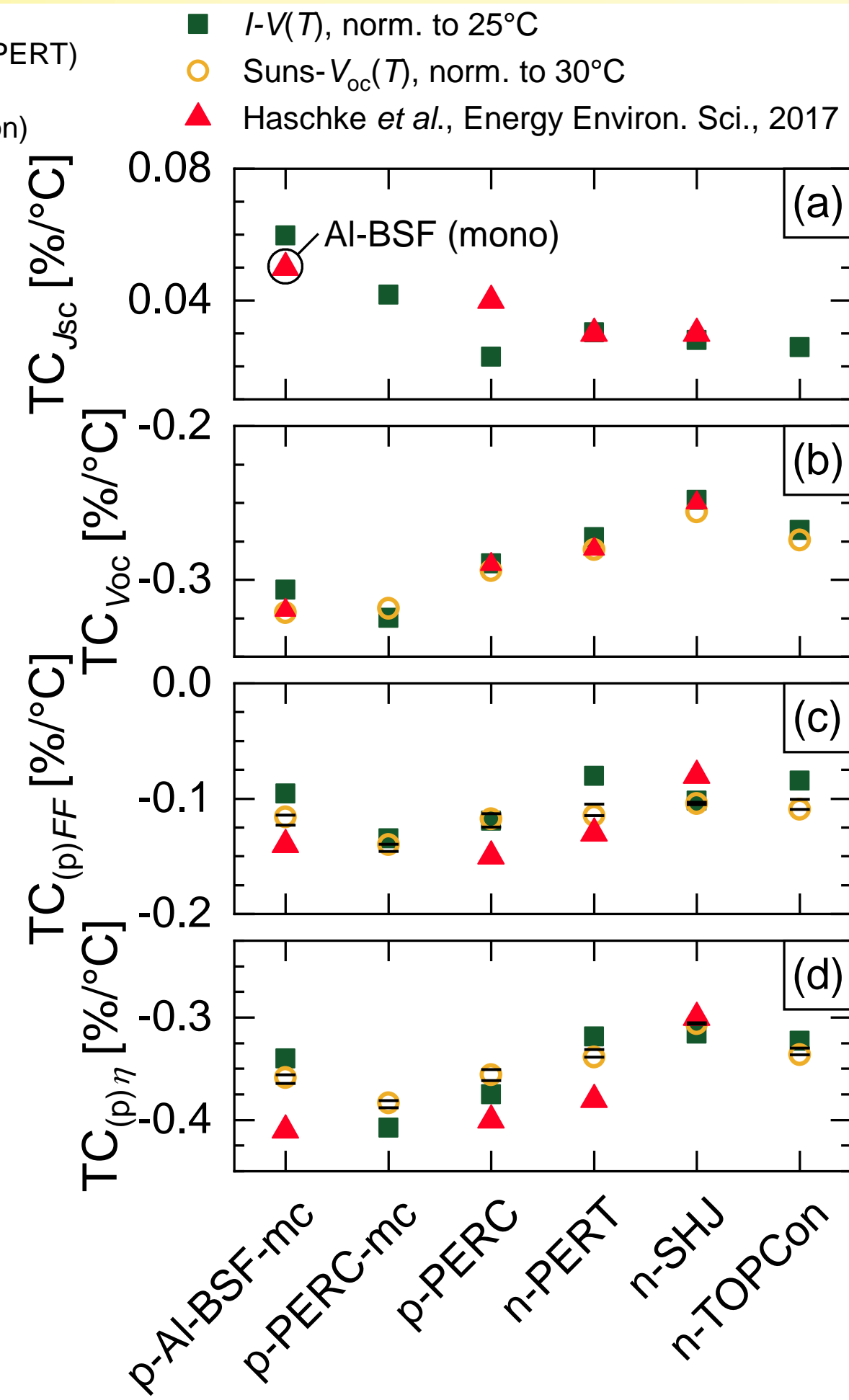


**Fig. 3.** Temperature coefficients of (a)  $J_{sc}$ , (b)  $V_{oc}$ , (c) (pseudo, p)  $FF$ , and (d) (pseudo, p)  $\eta$  extracted from the data obtained by  $Suns-V_{oc}(T)$  and  $I-V(T)$ .

$Suns-V_{oc}(T)$  vs  $I-V(T)$ :

- A good match for the temperature coefficient of  $V_{oc}$  ( $TC_{V_{oc}}$ ) values.
- Differences between the temperature coefficients of pseudo  $FF$  ( $TC_{pFF}$ ) and  $FF$  ( $TC_{FF}$ ) can be used to assess the contribution of the cell's series resistance.

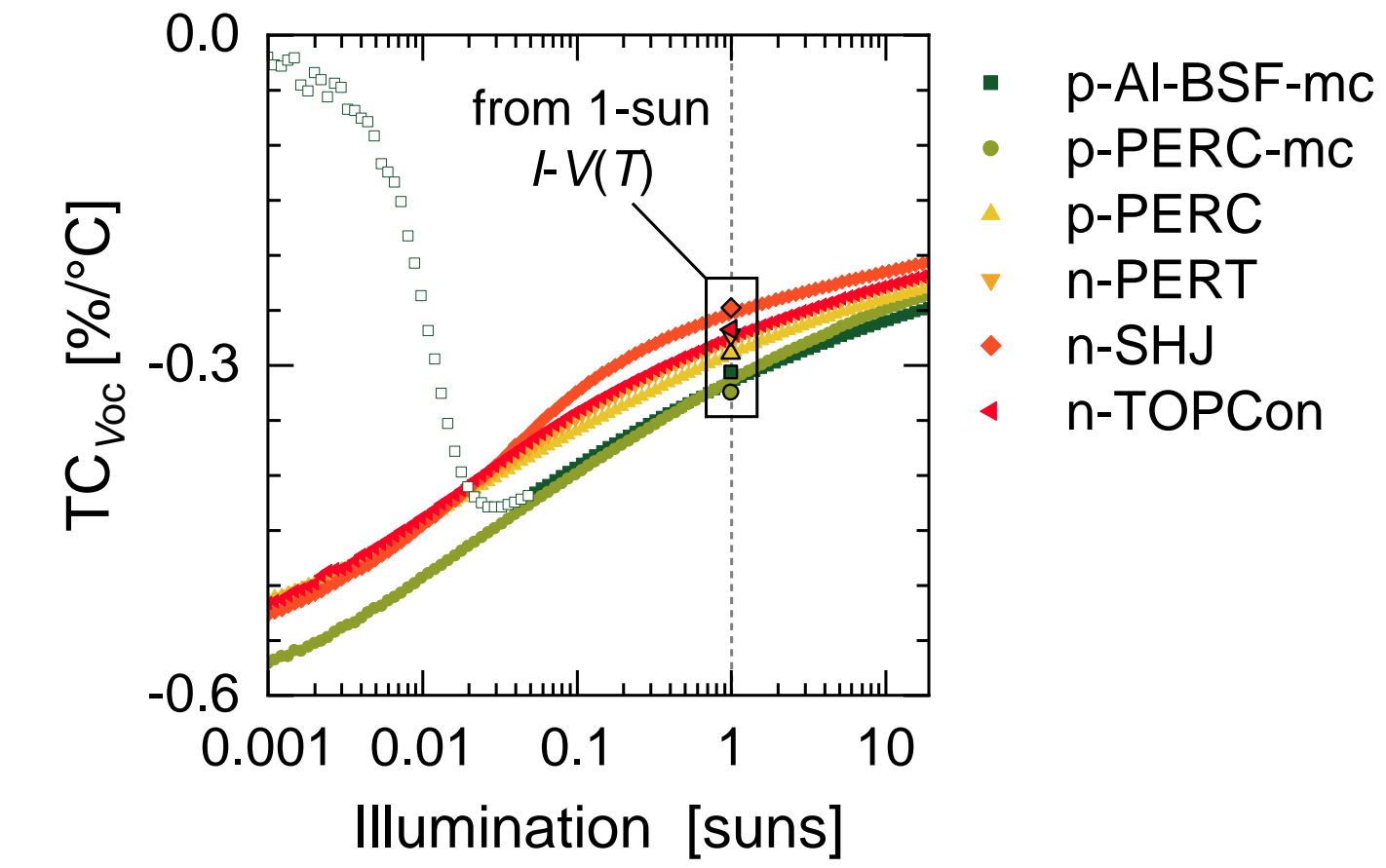


**Fig. 4.**  $TC_{V_{oc}}$  as a function of illumination intensity measured by  $Suns-V_{oc}(T)$ . Open symbols are the data points with R-squared of linear fits lower than 0.95.

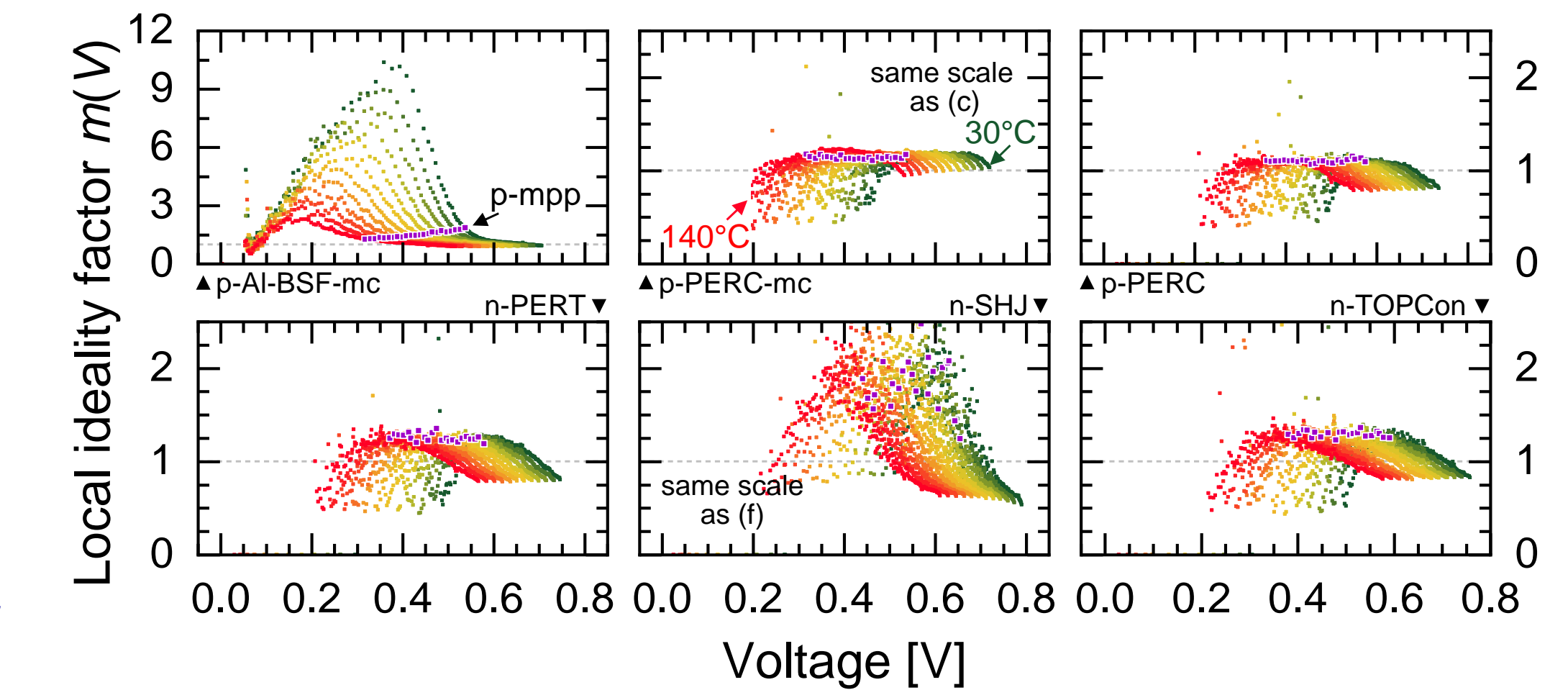


**Fig. 5.** Temperature-dependent ideality factor  $m(V)$  as a function of cell voltage measured by  $Suns-V_{oc}(T)$ .

- Local ideality factor ( $m$ ) decreases, and the peaks are shifted to lower voltage with increasing temperature, indicating an increase of the saturation current density of the second diode.
- Larger humps ( $m > 2$ ) in the case of p-Al-BSFmc cells indicate the effect of the cell's shunt resistance.

## Acknowledgement

This work was supported by the Australian Government through Australian Renewable Energy Agency [ARENA; project 2017/RND001]. The views expressed herein are not necessarily the views of the Australian Government, and the Australian Government does not accept responsibility for any information or advice contained herein.